

# Deposition of Cu and WO<sub>x</sub> films by thermal and hot-wire Chemical Vapor Deposition. Characterization and application of these films to microelectronics

Giorgos Papadimitropoulos <sup>1</sup>

Institute of Microelectronics, NCSR Demokritos, Patriarchou Grigoriou and Neapoleos Strs, 15310 Aghia Paraskevi, Greece  
[gpapad@imel.demokritos.gr](mailto:gpapad@imel.demokritos.gr)

**Abstract** It is presented for the first time a direct-liquid-injection hot-wire CVD system for copper chemical vapor deposition using hexafluoroacetylacetonate Cu(I) trimethylvinylsilane as precursor. The system enables: a) the selective chemical vapor deposition (SCVD) and b) the deposition of hot-wire CVD (HWCVD) Copper films. Moreover, it enables the deposition of tungsten oxide films, which adhere well on the oxidized Si substrates, by heating the tungsten filament only in an oxygen- or hydrogen-containing ambient. The producing films were used for several applications to microelectronics.

**Keywords** Thin Films, home-made system, Chemical Vapor Deposition, hot wire, copper, tungsten oxides

## 1 Introduction

In modern integrated circuit manufacturing copper has replaced the traditionally used aluminum for interconnects due to its lower bulk resistivity (1.8 vs 2.7  $\mu\Omega\cdot\text{cm}$ ) and higher electromigration resistance [1]. The use of copper in interconnects enables circuits to run faster and to be more reliably than when aluminum metalized [2]. Several methods have been developed to deposit copper layers such as electroplating [3], which is the most commonly used industrial method, and chemical vapor deposition (CVD) [1].

CVD methods ensure the deposition of conformal copper layers within small trenches and via holes without the need of current conductive seed layer, which is

<sup>1</sup> Dissertation Advisors: Angela Arapoyanni, Assoc. Professor and Dimitrios Davazoglou, Main Researcher

necessary in electroplating [3]. One of the main drawbacks in using CVD methods for copper deposition is that most of copper precursors are solid [1]. This renders these processes poorly repeatable, unreliable and with low growth rate. In order to overcome the above drawbacks metal organic (MO) liquid precursors were synthesized, in which the metal appears with an oxidation number equal to +1, and direct-liquid-injection (DLI) systems were developed [4]. It was shown in the past that using copper precursors with metal oxidation number +1 the selective CVD (SCVD) is possible under specific deposition conditions [1, 5-7].

During the first year of this thesis, the development of a novel home-made system for Chemical Vapor Deposition was fulfilled. It is a Low Pressure Chemical Vapor Deposition system with DLI (Direct Liquid Injection) of precursor equipped with a tungsten wire thus enabling the separate heating of the gas phase. The precursor used was the hexafluoroacetylacetonate Cu(I) trimethylvinylsilane, CupraSelect<sup>®</sup> which is liquid at room temperature. Using this home-made system, copper thin films were deposited thermally as well as with the aid of the tungsten hot-wire (Hot Wire Chemical Vapor Deposition, HWCVD) for various filament temperatures. The substrates used were W, TiN, SiLK, MPTMS and Low Temperature Oxide (LTO) on Si wafers. To be noted that HWCVD technique for copper deposition is presented for the first time in literature. In addition, the initial stages of Chemical Vapor Deposition were investigated on LTO and SiLK substrates activated with a self-assembled monolayer of 3-mercaptoptrimethylsilane (MPTMS). Besides, WO<sub>x</sub> films originating from the tungsten wire without the use of precursor, were deposited via the thermal evaporation technique. All the above samples were characterized with various methods such as SEM, AFM, XPS and XRD whereas the deposition rate and the resistivity were also studied. The presented thesis was accomplished with the applications of copper and tungsten oxide thin films. Therefore, new ways of metallization and copper nanoelectrodes with very high aspect ratio were suggested and developed. Furthermore, nanostructured WO<sub>x</sub> films were studied for applications in chemical sensing and organic light emitting diodes (OLEDs). Finally, hot wire copper nanoparticles were developed for application in organic memories of variable resistance.

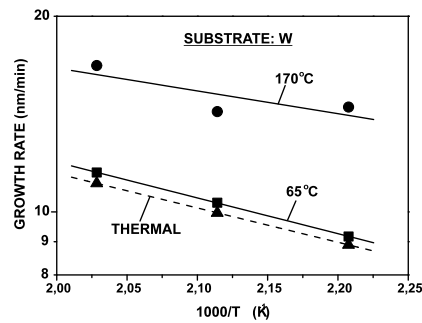
## 2 Copper films

Fig. 1 illustrates the home-made hot-wire CVD system developed here. The vertical type cold wall reactor is made of stainless steel and is equipped with a tungsten hot-wire to enable the separate heating of the gas phase.



**Fig. 1.** Home-made hot-wire CVD system for copper

In Fig. 2 the temperature variation of growth rate for HWCVD and thermally grown Cu films deposited on W is shown. It can be observed that the separate heating of the gas phase by the hot wire induces an increase of the deposition rate, which depends on the filament temperature and at 170 °C it increases by a factor of approximately one and a half. The kinetics of the reaction does not seem to be significantly influenced by the separate heating of the gas phase and, especially at 65 °C, the growth rate vs temperature variation is simply parallel shifted towards higher values as the filament temperature increases.



**Fig. 2.** Growth rate dependence on substrate temperature for HWCVD Cu films deposited on W-covered Si substrates. The corresponding dependence for thermally grown films is also reported in figure.

In Fig. 3 the growth rates of HWCVD Cu films deposited on TiN and SiLK<sup>®</sup>-covered Si substrates at temperatures of 180, 200 and 220 °C are shown. The deposition rate for thermal Cu films on TiN is also shown in figure (as mentioned before, thermal deposition on SiLK<sup>®</sup> did not occur at these temperatures). It is again observed a similar as in Fig. 2 trend i.e., heating the gas phase enhances growth rate and at higher filament temperatures the relative curves are parallel shifted towards higher values. However, the slope is different than that in Fig. 2 indicating that the substrate plays a role in the microscopic deposition kinetics.

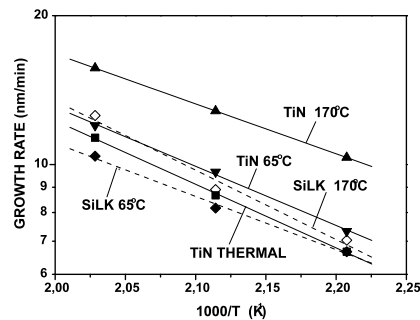


**Fig. 3.** Dependence of the growth rate of HWCVD Cu films on substrate temperature for films deposited on TiN and SiLK<sup>®</sup>-covered Si substrates. The corresponding variation for thermally grown films on TiN is also seen.

The composition analysis of HWCVD Cu films by XPS has revealed that except of cupric oxide detected at the outermost surfaces of all the samples, the bulk of films was quite pure as there were depths where there was no detectable oxygen and carbon was always below 4%. Carbon, oxygen and nitrogen from the substrate (SiLK<sup>®</sup>) became detectable as the interface region was approached. Traces of tungsten were detected in the interface region on all samples. This suggests that tungsten was deposited on the surface only at the beginning of the process. Fluorine appeared to be present in the substrate but was not detectable in the copper coating.

In Fig. 4 a compositional depth profile is shown for an approximately 150 nm thick HWCVD Cu sample on which the highest resistivity value was measured (14,2  $\mu\Omega\cdot\text{cm}$ ) deposited at substrate and filament temperatures of 180 and 170 °C, respectively. It is observed that the bulk of the film is mainly composed by Cu, the O content was very low (never exceeding 0,5%) but the C content at depths of 25 and 50 nm was measured near 4% before it drops at lower levels deeper in the film. These C concentration levels were the highest measured among the analyzed samples. The highest level of O was also measured on the same sample, near 0,5%. This contamination, as reported before, is probably due to the incomplete dissociation of the Cu-carrying clusters arriving on the surface, which decompose more difficulty than single precursor molecules. The number of such clusters should have to be almost equal to the number of precursor molecules dissociating on the substrate and this explains the high levels of contamination of this sample. All the other samples studied exhibited C contamination below 2% and O contamination at the limits of the measuring method.

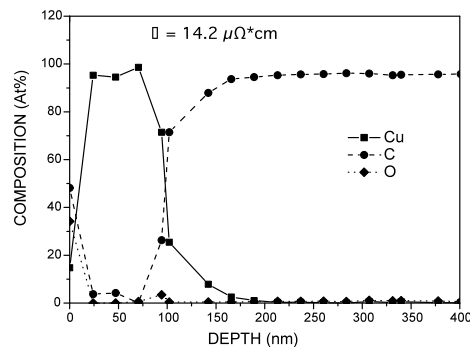


**Fig. 4.** Compositional depth profile of a 150 nm thick HWCVD Cu sample deposited on SiLK<sup>®</sup>.

In Fig. 5 SEM top views of thermally and hot-wire deposited Cu films on W covered substrates and at various temperature are shown. It can be observed that the surface morphology changes and the HWCVD films are more “grainy” and, therefore, rougher. A safe comparison of grain size cannot be made since samples produced by thermal CVD have elongated grains while in those by HWCVD the grains have a more spherical shape. It can be reported however that in Cu films grown thermally at 180 °C grains have sizes of the order of 100 nm, which increase with temperature to approximately 150 nm at 220 °C. HWCVD films grown with a filament temperature of 170 °C have grains with size increasing rapidly with substrate temperature from 100 to 400 nm for temperatures of 180 and 220

°C, respectively. The grain size in Cu films grown with filament temperature of 65 °C takes intermediate values near 200 nm.

In Fig. 6 the resistivity variation of Cu films thermally and hot-wire deposited on W and SiLK<sup>®</sup> covered substrates for filament temperatures of 65 and 170 °C are shown. Resistivities measured for Cu films grown on TiN either thermally or by HWCVD were in all cases slightly lower than those corresponding to W. It must be noted that resistivity values in Fig. 6 are overestimated because the thickness measurements by SEM were not very accurate.

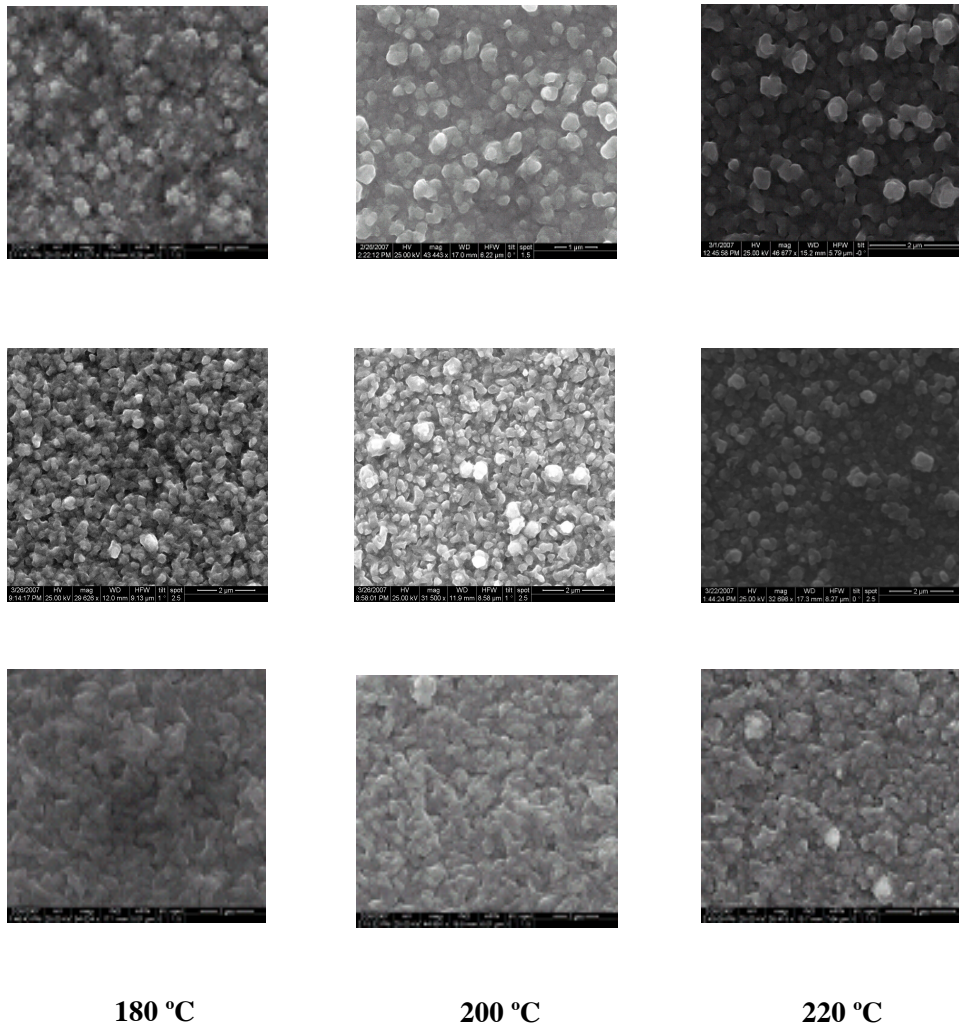


**Fig. 5.** SEM micrographs of the surface of HWCVD grown with filament temperatures of 170 (upper) and 65 °C (middle) and thermal Cu films (lower) deposited on W-covered Si substrates at 180, 200 and 220 °C.

Generally, Talystep measurements yielded lower thicknesses than those measured with SEM, i.e., lower films resistivities. Therefore, the highest resistivity values obtained are reported in Fig. 6. Another source of errors is that Cu films were not protected against oxidation after deposition (in several cases resistance measurements were made a few days after deposition) and this was confirmed by the XPS measurements. In any case, it is reasonable to believe that the general trends of the resistivity variation with the various parameters involved are preserved. It is observed that while the thermal Cu films grown on W have a resistivity of the order of  $2,5 \mu\Omega\cdot\text{cm}$  independent on deposition temperature, the HWCVD films at both filament temperatures exhibit higher resistivities which drop fast with substrate temperature towards the values for thermally grown films. These high resistivities, except of grain size effects are also related to the presence of C and O impurities as seen by the XPS measurements. However, no exact correlation between the concentration of a specific impurity and film resistivity could be obtained because, with the exception of the sample in Fig. 4, concentrations were varying within a very narrow range and resistivity values measured on the analyzed samples were all very near. Therefore, it is concluded that the presence of both kinds of impurities, C and O, affect film resistivity.

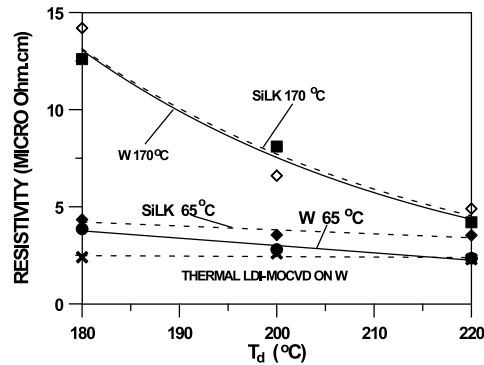


**Fig. 6.** Dependence of the Cu film resistivity on the temperature of deposition for HWCVD and thermal CVD films deposited on W and SILK® substrates. Resistivities for films grown on TiN were always slightly lower than those for W.

### 3 Tungsten Oxides

$\text{WO}_3$  films were deposited by heating a tungsten filament in a vacuum chamber (this is why the deposited films are named hereafter hot-wire tungsten oxide, hwWO, films) at temperatures lower than previously [4-7], namely temperatures of 650, 750 and 800 °C were used. During deposition the substrate remained at temperatures below 40 °C, depending on the duration of the last. After turning-off the filament, the sample was left to cool down to room temperature while the pressure used for the deposition was maintained. The cooling down was enduring several minutes.

The optical properties of hwWO samples were studied with SE measurements of  $\Psi$  and  $\Delta$  within the photon energy range 1,2 to 5 eV. In order to obtain the energy variation of the complex refractive index ( $\tilde{N}=n-ik$ ) of samples, theoretical spectra were synthesized and fitted to those experimentally recorded.

The former were synthesized with the aid of the effective medium theory (EMT) using two Lorentz oscillators to simulate the refractive index of the  $\text{WO}_x$  and voids. The adjustable parameters for fitting the theoretical to the experimentally recorded spectra were the parameters of the Lorentz oscillators, the film thickness and the volume fraction of voids. It must be noted here that two Lorentz oscillators with parameters very similar to those used here were used to obtain the refractive index dispersion of the LPCVD stoichiometric  $\text{WO}_3$  film. This result combined with Fourier transform infrared spectra, which revealed broad bands at wavenumbers near those corresponding to  $\text{WO}_3$ , indicates that hwWO films are composed by stoichiometric  $\text{WO}_3$ . The fitting was very satisfactory and  $n$  and  $k$  data for hwWO films deposited at 30 sec at various filament temperatures are shown in Fig. 7 together with those for a LPCVD  $\text{WO}_3$  deposited at 450 °C. It can be observed that  $n$  and  $k$  of hwWO films exhibit the same variation and features with those for the LPCVD  $\text{WO}_3$  film but are shifted towards lower values. These reduced values of  $n$  and  $k$  of hwWO films are responsible for their high optical transmission and low reflection. The Tauc band gap of LPCVD and hwWO films was found equal to 3.3 eV, which compares well with measurements reported in the literature [8].

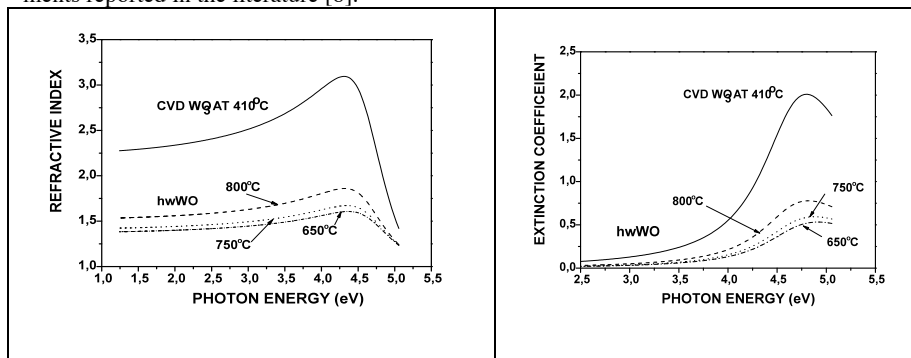


Fig. 7.  $n$  and  $k$  data for hwWO films deposited at 30 sec at various filament temperatures

#### 4 Applications to microelectronics

Planar Cu electrodes with high length (starting from 1 mm down to 50  $\mu\text{m}$ ) and fine widths dimensions (starting from 20  $\mu\text{m}$  and going down to 100 nm) were fabricated using selective chemical vapour deposition (SCVD) of the metal. For the fabrication, oxidized Si substrates were used on which a TiN layer was deposited and patterned either with PMMA. Then, Cu was deposited by SCVD on the exposed regions of the substrate only. Finally, the remaining polymers and the TiN were removed in acetone and by plasma etching, respectively. Due to the advanced CVD equipment used the above fabrication method proved to be robust, reproducible and with a high yield. The use of such equipment also assures a quite wide process window and inhibits the intrusion of other parameters which are known to destroy Cu SCVD.

In Fig. 8 SEM micrographs of interlacing electrodes formed on TiN covered by a PMMA layer and followed by SCVD of Cu at temperatures ranging between 100 and 160 °C are shown. PMMA was patterned with an electron beam (e-beam) machine and the minimum features go down to 100 nm wide. It can be observed that the selectivity is very good and is maintained at temperatures higher than other photoresists, i.e. AZ5214<sup>TM</sup>. This is probably related to the absence of photo-sensitive agents in the PMMA, as discussed

above. It must be noticed at this point that using SCVD of Cu on patterned polymers may yield features with dimensions deep in the nano-scale.

After SCVD of Cu, independent of the deposition temperature, the PMMA layer remains soluble in acetone and may be removed easily giving Cu patters with very low dimensions. The fabrication of planar Cu electrodes is accomplished with the etching of the TiN layer using the Cu features as hard mask. Although the etching process was not optimized, it was obtained readily. The process relies on the low volatility of the fluorinated Cu compounds that are formed on the surface of Cu during the initial stages of the etching process, which remain on top of the metal and protect it from further attack.

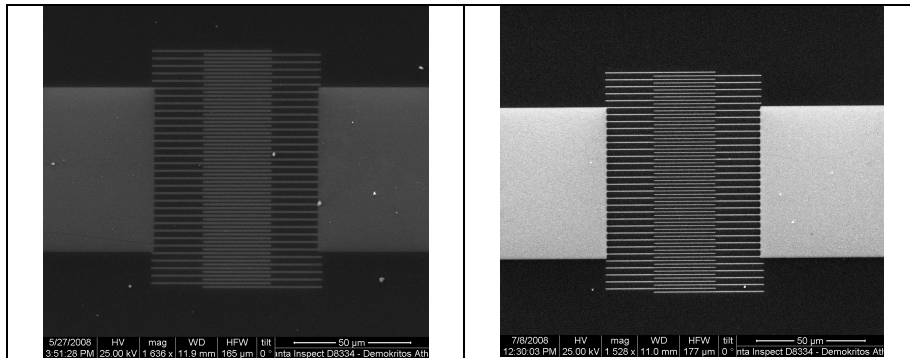


**Fig. 8.** SEM micrographs of interlacing electrodes formed on a TiN covered Si substrate by e-beam patterning a PMMA layer followed by SCVD of Cu at 100 (left) and 160 °C (right)

In this paragraph, we report the fabrication of a polymer light emitting diode (PLED) using nano-crystalline  $WO_x$  layers with various degrees of oxidation (various  $x$ ), as cathode interfacial layers in order to facilitate electron injection to the polymer light-emitting layer. It has already been reported that the reduction of  $WO_3$  results in the appearance of a narrow density of states band between the Fermi level and the lowest unoccupied molecular orbital (LUMO) (within the band gap) [9]. More specific, we explored this band as a manifold of hopping sites for enhancing electron injection and transfer from the Al cathode to the LUMO of the polymer layer and thus reducing the operating voltage and improving the overall PLED performance. In Fig. 9, the influence of  $WO_x$  (either fully oxidized or partially reduced) on the J-V and L-V characteristics of the fabricated PLEDs is shown. Devices with a thin film of reduced  $WO_x$  ( $x < 3$ ) exhibit a higher current density and luminance compared to both the reference device (without  $WO_3$ ) and the device with a thin film of oxidized  $WO_3$ . Obtained J and L values of  $\sim 2300$  A/m<sup>2</sup> and 1700 cd/m<sup>2</sup> compared to  $\sim 1700$  A/m<sup>2</sup> and 1200 cd/m<sup>2</sup>, respectively, at 15 V represent an increase of both the current density and the luminance of about 40 %. This improvement was, tentatively, attributed to the presence of a manifold of energy sites below the LUMO of reduced  $WO_x$  that may act as energetically favourable hopping sites for enhanced electron injection and transport, thus lowering the energetic barrier at the Al/polymer interface.



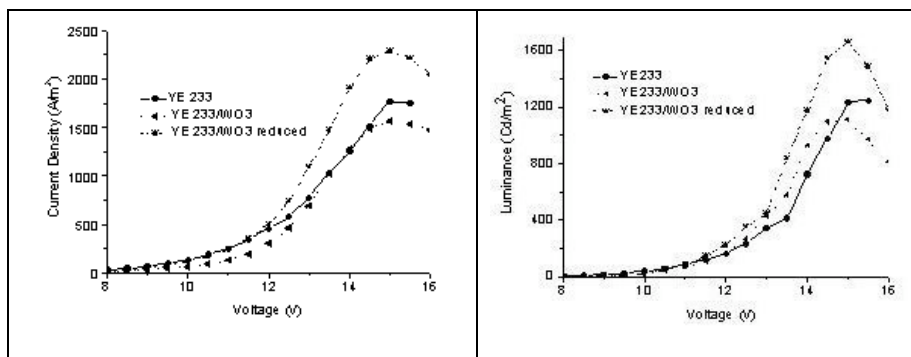


**Fig. 9.** J-V (left) and L-V (right) characteristics of the PLEDs.

Finally, hot wire copper nanoparticles were developed for application in organic memories of variable resistance. More precisely, we investigated the self-organization of Cu-NPs inside regioregular poly(3-hexylthiophene) (RR-P3HT) layers on quartz substrates. Due to the stacking properties of RR-P3HT layers, S atoms are presented at the surface of the layers. Recently, we have demonstrated that S atoms can act as coordination sites for Cu atoms after physical vapor deposition (PVD) and subsequent annealing. Here, we report on the fabrication of hot-wire chemical vapor deposition (HW-CVD) Cu-NPs embedded in organic materials leading to memory effects. It is believed that HW-CVD will create a finer distribution of Cu-NPs that allows avoiding the post-deposition annealing (PDA) step which cause metal atoms diffusion into the bulk of organic semiconductor layer. Typical I-V characteristics exhibiting switching from a high resistivity state (HRS) to a lower resistivity state (LRS) are presented in figure 10. Switching occurs at about  $\sim +4V$  after sequential voltage sweeps causing 3 orders of magnitude increase in current.

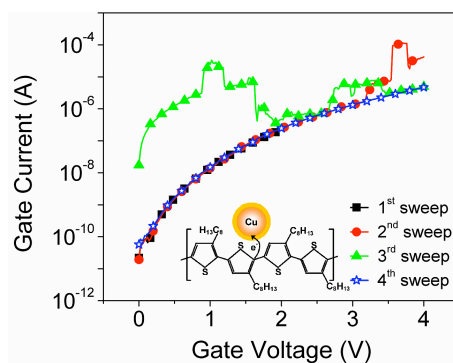


**Fig. 10.** Typical I-V characteristics showing resistivity switching. Inset, demonstrates a possible scenario for resistivity switching.

## 5. References

1. Kodas T, Hampten-Smith M, "The Chemistry of Metal CVD", VCH, Weinheim, 1994
2. Edelstein D, Heidenreich J, Goldbatt R, Cote W, Uzoh C, Lusting N, Roper P, McDevitt T, Motsiff W, Simon A, Ducovic J, Wachnick R, Rathor H, Schulz R, Su L, Luce S, Slattery J, Tech. Digest IEEE Int. Electron Devices Mtg., (1998) pp. 773
3. Andricacos P, The Electrochem. Soc., "Interface", (Spring 1999) pp. 32
4. J. Liu, Z. Zhang, Y. Zhao, X. Su, S. Liu and E. Wang, *Small*, 2005, 1, pp. 310-313
5. J. Zhou, Y. Ding, S. Z. Deng, L. Gong, N. S. Xu and Z. L. Wang, *Adv. Mat.*, 2005, 17, pp. 2107-2110
6. J. Liu, Y. Zhao and Z. Zhang, *J. Phys.: Cond. Matter*, 2003, 15, L453-L461
7. G. Cu, B. Zheng, W. Q. han, R. Siegmar and J. Liu, *Nano Lett.*, 2002, 2, pp. 829
8. D. Gogova, K. Gesheva , A. Szekeres , and M. Sendova-Vassileva , Structural and Optical Properties of CVD Thin Tungsten Oxide Films, *phys. stat. sol. (a)* 176, 1999, pp. 969-972
9. R.J. Colton, A.M. Guzman, J.W. Rabalais, *J. Appl. Phys.* 49 (1978) pp. 409-416